A Thermodynamic Comparison of HPr Proteins from Extremophilic Organisms[†]

Abbas Razvi[‡] and J. Martin Scholtz*[,‡,§]

Department of Biochemistry and Biophysics, Texas A&M University, and Department of Molecular and Cellular Medicine, Texas A&M University College of Medicine, 440 Reynolds Medical Building, College Station, Texas 77843-1114

Received January 6, 2006; Revised Manuscript Received February 9, 2006

ABSTRACT: A thermodynamic stability study of five histidine-containing phosphocarrier protein (HPr) homologues derived from organisms inhabiting diverse environments is described. These HPr homologues are from *Bacillus subtilis* (*Bs*), *Streptococcus thermophilus* (*St*), *Bacillus staerothermophilus* (*Bst*), *Bacillus halodurans* (*Bh*), and *Oceanobacillus iheyensis* (*Oi*). Analyses of solvent and thermal denaturation experiments provide the cardinal thermodynamic parameters, like ΔG, ΔH, ΔS, T_m, and ΔC_p, that characterize the conformational stability for each homologue. The homologue from *Bacillus staerothermophilus* (*Bst*HPr) was established as the most thermostable homologue and also the homologue with highest ΔG at all temperatures. A good correlation between habitat temperature of the organism and thermal stability of the protein is also seen. Stability curves (ΔG vs T) for every homologue are also reported; these reveal very similar ΔC_p and temperature of maximum stability (T_S) values for all HPr homologues. Stability curves show that the higher thermal stability of some homologues is not a result of change in curvature of the curve or a shift to higher temperature, but rather a displacement of the stability curves to higher ΔG values. Stability curves also allowed estimation of ΔG at habitat temperature of the organisms, and we find good agreement between homologues. Electrostatic contributions to stability of each homologue were investigated by measuring stability as a function of varying pH and NaCl concentration, and our results suggest that most HPr homologues share similar electrostatic contributions to stability.

The folded conformation of a protein is stabilized by various forces (including hydrophobic, electrostatic, and hydrogen bonding interactions) acting to offset alternative forms, which are favored by conformational entropy. Although our understanding of these forces has improved significantly (*1*, *2*), a complete knowledge of the balance of forces and the interplay between them is still lacking. Studies of proteins derived from extremophilic organisms may provide additional insights into forces stabilizing the native conformation of proteins. The term ‘extremophiles’ has been used to describe organisms that have adapted to live at extremes of temperature, salinity, pH pressure, and so forth. Numerous studies have focused on the ability of proteins from these organisms to fold and function at the extreme environmental conditions (*3*−*8*). Several hypotheses have been proposed to explain the enhanced stability of these proteins, including an increased number of hydrogen bonds (*9*, *10*), improved core packing (*11*), optimized electrostatics (*12*), and improved hydrophobic interactions (*13*). Although these and other modes of stabilization apply in many cases, a unifying description for conferring thermostability on a protein remains elusive (*14*).

Thermophilic adaptations are of particular interest because survival in extremes of temperature most likely requires that the proteins themselves become more thermostable, (*15*), whereas in other kinds of stress (like pH, osmotic), the organisms can survive by ‘avoiding’ these stress factors by compensatory mechanisms such as pH regulation (*16*) or synthesis of low molecular weight ‘osmoprotectants’ (*17*−*19*). Proteins from thermophiles and extremophiles are also of interest to biotechnology because these proteins are more tolerant to harsher conditions of temperature, solvent composition (presence of additive or organic solvents), pH, and salinity (*20*, *21*), which are advantageous because they provide for higher reaction rates, higher substrate concentrations, and lower viscosity while also reducing chances of microbial contamination. To confer these advantages on proteins of mesophilic origin, directed evolution (*22*, *23*) and other protein engineering (*24*) experiments have been used, but a complete understanding of the enhanced stability is lacking. Proteins from extremophilic organisms provide good model systems to study the forces responsible for protein stability by comparing them with homologues derived from species inhabiting more moderate habitats (for example see refs *25*−*27*). These studies often use detailed thermodynamic analysis of the homologous pair of proteins under a wide range of solution conditions together with comparison of their three-dimensional structures (*28*), in attempts to rationalize the differences in stability.

Here, we provide a detailed thermodynamic analysis of five histidine-containing phosphocarrier protein (HPr)[1] homologues all derived from gram-positive bacteria, which

[†] Supported by the NIH (Grant GM52483) and Robert A. Welch Foundation (Grant BE-1281).

* To whom correspondence should be addressed. Phone, (979) 845-0828; fax, (979) 847-9481; e-mail, jm-scholtz@tamu.edu.

[‡] Department of Biochemistry and Biophysics, Texas A&M University.

[§] Department of Molecular and Cellular Medicine, Texas A&M University College of Medicine.

10.1021/bi060038+ CCC: $33.50
Published on Web 03/14/2006

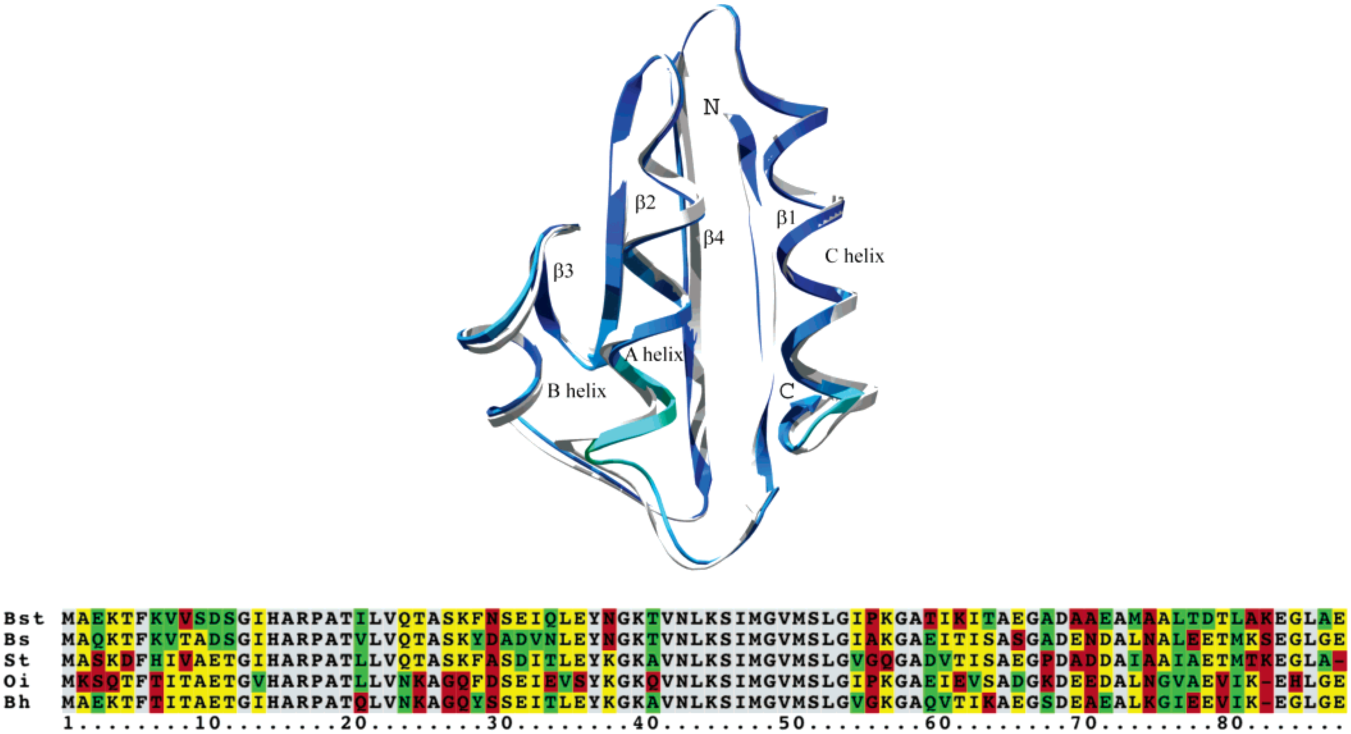

FIGURE 1: Ribbon diagram showing Cα superposition of *Bs*- and *Bst*HPr structures. The *Bst*HPr ribbon has been colored to depict regions of high Cα rmsd in cyan and low rmsd in dark blue. The PDB files 2HPR (*Bs*) and 1Y4Y (*Bst*) were used in Swiss-PDB viewer program (*49*) to prepare the figure. A sequence alignment for *Bst*-, *Bs*-, *St*-, *Oi*-, and *Bh*HPr is also shown revealing a sequence identity ranging from a high 72% (*Bst*- and *Bs*HPr) to low 60% (*Oi*- and *Bs*HPr) between the homologues. The sequences are shaded to indicate identical (gray and yellow), semiconserved (green), or nonconserved (red) residues among proteins.

inhabit very different environments. These HPr homologues are from *Bacillus subtilis* (*Bs*), *Streptococcus thermophilus* (*St*), *Bacillus staerothermophilus* (*Bst*), *Bacillus halodurans* (*Bh*), and *Oceanobacillus iheyensis* (*Oi*). *B. subtilis* is a mesophile (*29*), *S. thermophilus* (*29*) and *B. staerothermophilus* (*30*) are moderate thermophiles, *B. halodurans* is a haloalkaliphilic thermophile (*31*, *32*), and *O. iheyensis* is an extremely halotolerant alkaliphile (*33*). HPr is a small (∼88 amino acid) monomeric protein that is involved in the PTS sugar transport pathway in bacteria (*34*). The HPr protein exhibits reversible two-state folding (*35*−*38*) in both thermal and solvent denaturation experiments under a variety of conditions, and the other homologues described here have similar features. The availability of high-resolution crystal structures for two homologues (*38*, *39*), together with their relatively small size, lack of disulfide bonds, and prosthetic groups, makes these proteins good model systems for folding studies. The HPr homologues show high sequence identity (see Figure 1 for sequence alignment) and yet show diversity in their thermodynamic behavior. The detailed thermodynamic characterization of HPr homologues undertaken here should be a useful step toward revealing features that enable these proteins to function in their habitat conditions.

EXPERIMENTAL PROCEDURES

Cloning of HPr Homologues. Plasmids for the expression of the HPr homologues from *Bs* and *Bst* have been described previously (*40*, *41*). For the other HPr homologues (*St*, *Bh*, and *Oi*), the HPr gene was cloned into appropriate vectors to create plasmids for protein expression.

The *St*HPr gene was cloned into the pLOI 1803 vector using a PCR-based cloning method by a modification of the method of Howorka and Bayley (*42*). To obtain the gene coding for *St*HPr, genomic DNA was purified from *S. thermophilus* cells, which were obtained from the ATCC (BAA-491). The freeze-dried culture was rehydrated with trypticase soy broth (BD 236950) and supplemented with 5% (v/v) defibrinated sheep blood. A 30 mL culture (grown for 12−16 h) was used to prepare genomic DNA using standard methods (*43*). The genomic DNA was used as a template in a PCR reaction to amplify the HPr gene. The primers used for *St*HPr gene amplification had overhangs that are complementary to the vector sequence (*St*HPr gene amplification sense primer: <u>G GGA ATG ATG AAC</u> ATG GCT TCT AAA GAT TTC, the underlined bases indicate the overhang region complementary to the vector sequence); similarly, the primers used to amplify the pLOI 1803 vector DNA had overhangs complementary to the *St*HPr gene (sense primer for vector amplification: <u>GGA TTG GCA TAA</u> TGG GAA ACG CAA TCC, underlined bases indicate overhang region complementary to the *St*HPr gene).

The HPr gene was amplified by PCR using Taq polymerase, and the vector DNA was amplified using Herculase

[1] Abbreviations: HPr, Histidine-containing phosphocarrier protein; PTS, PEP:glycose phosphotransferase system; *Bs*, *Bacillus subtilis*; *Bst*, *Bacillus staerothermophilus*; *St*, *Streptococcus thermophilus*; *Bh*, *Bacillus halodurans*; *Oi*, *Oceanobacillus iheyensis*; TE, Tris EDTA; ΔG, free energy of stabilization; T_m, melting temperature or the temperature at midpoint of the unfolding transition; ΔH_m, van't Hoff enthalpy at T_m; ΔC_p, change in heat capacity associated with protein unfolding; ΔASA, change in solvent accessible surface area associated with protein unfolding; CD, circular dichroism spectroscopy; GuHCl, guanidinium hydrochloride; T_S, temperature of maximum stability or the temperature where change in entropy between native and denatured states is zero; ΔG_S, free energy of stabilization at T_S; T_E, environment or habitat temperature of an organism; ΔG_E, free energy of stabilization at T_E.

polymerase mix from Stratagene. Success of the PCR was confirmed by analysis of the products on agarose gels. The PCR products from both reactions were then mixed and transformed into chemically competent XL1-blue *Escherichia coli* cells (Stratagene). The transformants were tested for the presence of desired plasmid by colony PCR. Finally, the plasmid DNA was sequenced to confirm the presence and correct orientation of the *St*HPr insert.

The *Oi*HPr gene was cloned into the pUC (HPr) (*40*) vector using the same four-primer cloning method used for cloning the *St*HPr gene. The gene coding for *Oi*HPr was obtained from *O. iheyensis* genomic DNA, which was purified from cultures obtained from the DSMZ (Braunschweig, Germany). This culture was rehydrated in marine broth (BD 2216), and a 30 mL culture of these cells was used for genomic DNA preparation, employing the standard methods used earlier (*43*), except the lysis step of the cells had to be performed by passage through a french press at 1200 psi. This was necessary because the standard alkaline lysis procedure was not successful in lysing these bacteria. The primers used for *Oi*HPr gene amplification (GT TGG GGA AAT ACA ATG AAA TCA CAA ACA TTT AC) and vector amplification (GGT GAA TAG CCC GGG TAG CCA AAG) were designed according to methods used for the *St*HPr cloning. The PCR amplification reaction, subsequent transformation, and screening protocols used were identical to those used for cloning of the *St*HPr gene.

The gene for *Bh*HPr was cloned into the pLOI 1803 (*41*) vector using restriction enzyme digests and subsequent ligation into the vector DNA. The genomic DNA for this bacterium was prepared according to methods described for *S. thermophilus* from a culture obtained from the ATCC (BAA-125). The primers used for *Bh*HPr gene amplification had overhangs that were the recognition sequence for restriction enzyme Bgl II (GAG TAGA TCT ATG GTT GAA AAA CAA G, the underlined bases indicate recognition site for Bgl II); similarly, the primers used for amplification of vector DNA had overhangs which coded for the recognition sequence of Bgl II (G AGT AGA TCT TGG GAA ACG CAA TC).

The enzymes and the reaction conditions used for both *Bh*HPr insert and vector amplifications were the same as described for *St*- and *Oi*HPr. The PCR products were purified using the QIAquick PCR Purification Kit (Qiagen). The restriction digest with Bgl II was performed using conditions recommended by the enzyme manufacturer (NEB). The digested DNA for both insert and vector reactions was treated with Shrimp Alkaline Phosphatase (SAP) for 15 min at 37 °C followed by inactivation. These reaction products were purified and the products eluted in deionized water followed by concentration to 10 μL. The purified reaction products were used to set up a ligation reaction with T4 DNA ligase (Promega). The ligation reaction was used to transform 80 μL of chemically competent XL1 blue *E. coli* cells. The transformants obtained were screened for the presence of plasmid with the *Bh*HPr insert according to methods described above. The positive clones were processed further to obtain plasmid DNA, which was sequenced to confirm the presence of the correct plasmid with the *Bh*HPr insert in the proper orientation.

Protein Expression and Purification. The ES7R strain of *E. coli* was used for expression of the HPr proteins (*44*). All HPr homologues were expressed and purified using the protocol for *Bst*HPr published earlier (*38*) with slight modifications. The yield of pure protein in each case was approximately 60−70 mg/L of culture. The yield for *Oi*HPr was lower partly due to accumulation of some protein in the inclusion bodies; however the yield was sufficient (30 mg/L of culture) for our purposes.

The purification protocol for HPr homologues differed from that for *Bst*HPr at two steps, (a) the pH of the TE buffer (10 mM Tris and 1 mM EDTA) used and/or (b) the ion exchange step. For purification of *Bs*- and *Oi*HPr, identical protocols were used. The pH of the 2× TE buffer used for this protocol was 7.2 instead of 8.4, which was used for purification of *Bst*HPr. In the ion exchange step, the resin was washed additionally with 2 bed volumes of 0.2 M NaCl in 2× TE and the eluate was pooled with the flow through fraction collected earlier. For the purification of *St*HPr, the pH of the 2× TE buffer was adjusted to 7.2 and the ion-exchange resin was washed with 2 bed volumes of 0.1 M NaCl in 2× TE. For purification of *Bh*HPr, the ion-exchange resin was washed with 2 bed volumes of 0.15 M NaCl in 2× TE.

Thermodynamic Stability Measurements. The circular dichroism signal at 222 nm was used to monitor the unfolding transitions of the proteins with either an Aviv 62DS or Aviv 202SF spectropolarimeter equipped with temperature control and stirring units, according to methods described earlier (*38*, *45*). The data from solvent and thermal denaturation experiments were analyzed according to methods described earlier (*45*). The experiments studying ionic strength dependence of protein stability were performed using urea as the denaturant, and both the buffer (10 mM sodium phosphate at pH 7) and the urea solutions contained identical concentrations of NaCl. Similarly, the experiments studying pH dependence of protein stability were done using urea as the denaturant. In this case, the urea stock and protein solution in the cuvette were prepared in the same buffer mix of sodium citrate, sodium phosphate, and sodium borate (final concentration of 10 mM) adjusted to the same pH.

Stability Curves. To obtain stability curves (*46*) for the HPr homologues or their variants, the ΔG from urea denaturation experiments at temperatures between 5 and 50 °C were combined with data from the transition region of a thermal denaturation experiment and fit by a modified form of the Gibbs−Helmholtz equation (eq 1) according to methods of Pace and Laurents(*47*):

$$\Delta G(T) = \Delta H_m(1 - T/T_m) - \Delta C_p[(T_m - T) + T\ln(T/T_m)] \quad (1)$$

where, $\Delta G(T)$ is the free energy at a temperature T, ΔH_m is the van't Hoff enthalpy at T_m, ΔC_p is the change in heat capacity associated with unfolding, and T_m is the melting temperature or the temperature at the midpoint of the transition.

Sequence Alignments. Alignments were generated using CLUSTALW program (*48*). The alignment was shaded using the BOXSHADE tool available from the Biology Workbench Web site (http://workbench.sdsc.edu).

RESULTS

Conformational Stability of HPr Homologues. The conformational stability of all the proteins in this study was

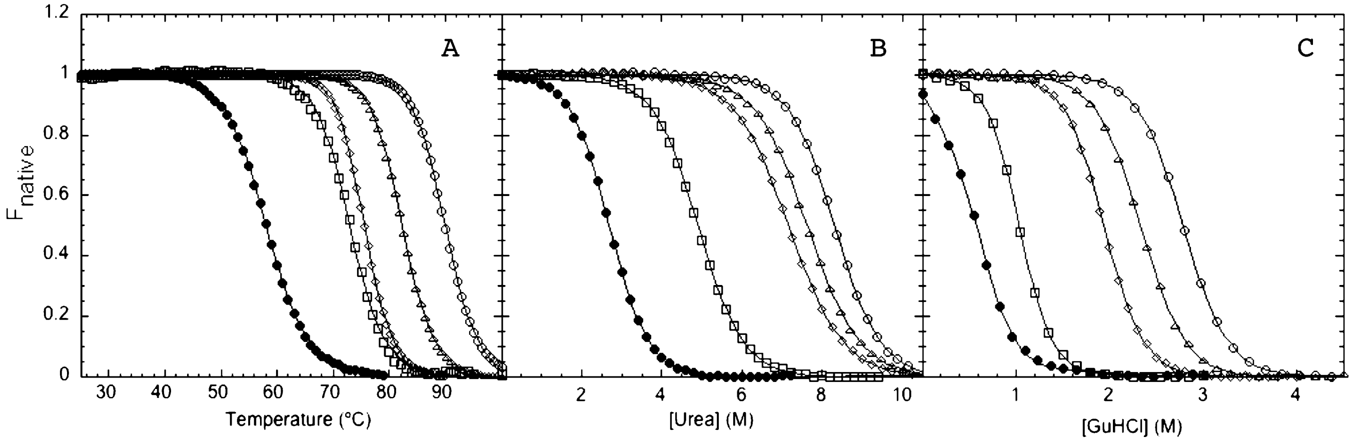

FIGURE 2: Representative thermal (A), urea (B), and GuHCl denaturation (C) unfolding curves for *Oi*- (●), *Bs*- (□), *St*- (◊), *Bh*- (△), and *Bst*HPr (○). All experiments were performed in 10 mM sodium phosphate at pH 7, and the data in panels B and C were collected at 25 °C. Data from CD at 222 nm were normalized to native fraction using equations described in Experimental Procedures.

Table 1: Parameters Characterizing Urea, GuHCl, and Thermal Denaturations for *Oi*-, *Bs*-, *St*-, *Bh*-, and *Bst*HPr at pH 7[a]

	urea denaturation		GuHCl denaturation			thermal denaturations	
protein	ΔG (kcal mol^{-1})	m value[b] (kcal mol^{-1} M^{-1})	ΔG (kcal mol^{-1})	m value[c] (kcal mol^{-1} M^{-1})	$\Delta\Delta G_{\text{urea}-\text{GuHCl}}$ (kcal mol^{-1})	T_m (°C)	ΔH_m[d] (kcal mol^{-1})
***Bs*HPr**	5.0 (±0.2)	1.08	3.4 (±0.1)	3.28	1.6	73.0 (±0.6)	77
***St*HPr**	6.3 (±0.1)	0.86	5.4 (±0.1)	2.75	0.9	75.6 (±0.1)	95
***Bst*HPr**	8.2 (±0.2)	0.98	6.7 (±0.1)	2.43	1.5	88.3 (±0.8)	99
***Oi*HPr**	3.4 (±0.2)	1.27	1.4 (±0.1)	2.56	2.0	58.0 (±0.8)	59
***Bh*HPr**	6.8 (±0.1)	0.90	5.3 (±0.2)	2.36	1.5	82.3 (±0.6)	87

[a] All experiments were performed in 10 mM NaPi, pH 7, and the solvent denaturation experiments were performed at 25 °C. All values reported are averages of results from multiple experiments, and the values in parentheses are the measured standard deviations. [b] Standard deviations for m value from urea denaturations were ≤5%. [c] Standard deviations for m value from GuHCl denaturations ≤5% [d] Standard deviations in ΔH_m were usually ≤10% of the average value reported.

determined through the analysis of solvent (urea or GuHCl) and thermal denaturation curves, where CD spectroscopy at 222 nm was used as a probe to follow the conformation of the protein. The transitions from the native to denatured conformation in all cases were cooperative with flat native and denatured state baselines. In case of thermal denaturations, at least 90% reversibility was observed, and in both cases, the transitions were independent of protein concentration over the studied concentration range of 5−50 μM. Typical results from thermal, urea, and GuHCl denaturation experiments are presented in Figure 2, and the thermodynamic parameters obtained for each HPr homologue are presented in Table 1.

The HPr homologues show a range of ∼30 °C in T_m (Figure 2A), with *Oi*HPr having the lowest T_m at 58 °C and *Bst*HPr having the highest T_m at 88.3 °C. The order of thermostability from thermal denaturation experiments is *Bst* > *Bh* > *St* > *Bs* > *Oi*HPr. The ΔH values for all the proteins are also listed in Table 1; again, *Oi*HPr has the lowest ΔH and *Bst*HPr has the highest. The results from urea denaturation (Figure 2B) show a similar trend in stability (ΔG) for the HPr proteins. *Bst*HPr is the most stable homologue and *Oi*HPr the least stable, with a difference of ∼5 kcal mol^{-1} at 25 °C. The m values for urea denaturation are also very similar for most of these proteins (∼1.0 kcal mol^{-1} M^{-1}), with only *Oi*HPr showing a slightly higher m value (1.3 kcal mol^{-1} M^{-1}). GuHCl denaturation experiments were also performed (Figure 2C) and returned a ΔG of 6.8 and 1.4 kcal mol^{-1} for *Bst*- and *Oi*HPr, respectively. As in the case of urea denaturation experiments, the m values for the proteins are very similar, around 2.7 kcal mol^{-1} M^{-1}. *Bs*HPr appears to be the outlier with an m value of 3.3 kcal mol^{-1} M^{-1}. As one estimate of potential difference in electrostatic interactions, we can also look at the differences in stability estimated from GuHCl and urea denaturation experiments ($\Delta\Delta G_{\text{urea}-\text{GuHCl}}$). We find that $\Delta\Delta G_{\text{urea}-\text{GuHCl}}$, is the lowest for *St*HPr and highest for *Oi*HPr at 0.9 and 2.0 kcal mol^{-1}, respectively, while the other HPr homologues have a $\Delta\Delta G_{\text{urea}-\text{GuHCl}}$ value close to 1.5 kcal mol^{-1}. These results will be discussed in more detail below.

Stability Curves for HPr Homologues. Protein stability curves, first described by Becktel and Schellman (*46*), define the variation of conformational stability (ΔG) with temperature. Here, we use the method of Pace and Laurents (*47*) to construct such curves by combining data from both thermal and solvent denaturation experiments. We find that the HPr homologues have similar stability curves that are simply shifted up or down on the ΔG axis. The stability curve for *Bst*HPr is shifted up the most, and the lowest curve is for *Oi*HPr (Figure 3). A fit of the modified Gibbs−Helmholtz relationship (eq 1) to the data provides the parameters shown in Table 2. As expected from the shape of the curves, the values of ΔC_p and T_S (temperature of maximum stability or the temperature where change in entropy between native and denatured states is zero) are very similar among the homologues (Table 2). The availability of the stability curves allows us to calculate ΔG at the habitat or environment temperature (ΔG_E), and we find that the ΔG_E values for the HPr homologues are very similar (∼5.0 kcal mol^{-1}), except for *Oi*HPr which is lower (3.2 kcal mol^{-1}).

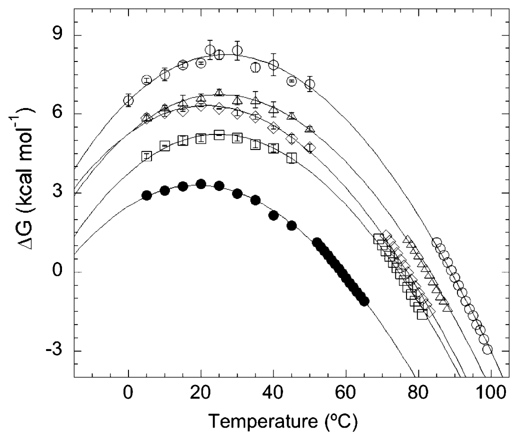

FIGURE 3: Stability curves (ΔG versus T) for the for *Oi*- (●), *Bs*- (□), *St*- (◇), *Bh*- (△), and *Bst*HPr (○) proteins. The data at lower temperatures (0−50 °C) are from results of urea denaturation experiments, and the data at higher temperatures are from thermal denaturation experiments in the absence of urea. Curves through the data are fits of eq 1. The error bars for data in the low-temperature range depict standard deviation from repeated measurements; for some data, error bars are smaller than the symbol. The parameters derived from Gibbs−Helmholtz analyses (eq 1) are presented in Table 2.

Table 2: Parameters Characterizing the Stability of the *Oi*-, *Bs*-, *St*-, *Bh*-, and *Bst*HPr Proteins[a]

protein	ΔG_S[b] (kcal mol^{-1})	T_S[c] (°C)	ΔG_E (kcal mol^{-1})	T_E (°C)	ΔC_p[d] (kcal mol^{-1} K^{-1})
***Bs*HPr**	5.2	24.1	4.8	25	1.3
***St*HPr**	6.3	22.2	4.6	50	1.3
***Bst*HPr**	8.2	24.8	5.0	65	1.3
***Oi*HPr**	3.3	20.2	3.2	20	1.2
***Bh*HPr**	6.7	25.5	4.9	55	1.3

[a] ΔG_S is the stability at T_S, which is the temperature of maximal stability; ΔG_E is the stability at environment temperature of the organism (T_E). Values for ΔC_p are best-fit estimates from fits of eq 1 to the data defining the stability curve. The values of ΔG_S and ΔG_E are from modified forms of eq 1; values of T_E were those reported in the literature (adapted from refs *29, 30, 32, 33*). [b] Standard deviation in ΔG values obtained from fits of eq 1 ranged from 0.1 to 0.2 kcal mol^{-1}. [c] Standard deviation in temperature estimates from fits of eq 1 were usually 0.1 °C. [d] Errors in ΔC_p estimates are usually 10%.

Electrostatic Contributions to Protein Stability: *Salt and pH Effects on Protein Stability*. To explore how electrostatic interactions contribute to the stability of the HPr proteins, the conformational stability was determined as functions of ionic strength and pH. Urea denaturation experiments were performed at NaCl concentrations between 0 and 1.2 M (Figure 4). The HPr homologues show a common trend in stability in response to added NaCl. At concentrations below 0.3 M, all homologues lose stability, while above 0.3 M, all proteins gain stability. The relative magnitudes of change in stability for the different HPr homologues in both concentration domains are similar, except for *Bs*HPr which shows a larger drop in stability at low NaCl concentration.

The effect of pH on the stability of the HPr homologues was investigated by performing urea denaturation experiments at various pH values from 3 to 10 (Figure 5). The *Oi*HPr protein was completely unfolded below pH 4 and above pH 9 at 25 °C, and thus, we could not collect any useful data at these pH values. Three of the five HPr homologues (*Bs*-, *Bst*-, and *Oi*HPr) show maximal stabilities at neutral pH, while *St*- and *Bh*HPr are most stable near pH

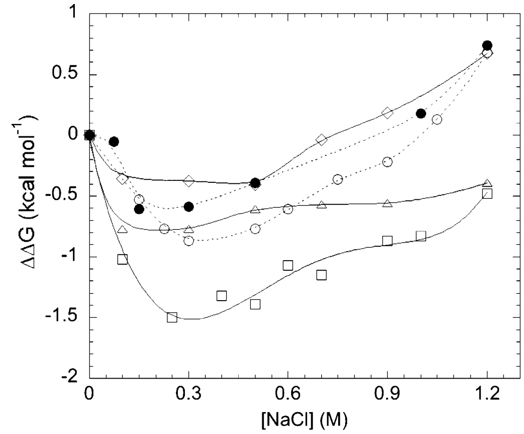

FIGURE 4: The changes in conformational stability ($\Delta\Delta G$) as a function of [NaCl] for the *Oi*- (●), *Bs*- (□), *St*- (◇), *Bh*- (△), and *Bst*HPr (○) proteins. Stability measurements were made using urea denaturation experiments performed in increasing [NaCl] at 25 °C in 10 mM NaPi, pH 7. The stability data obtained were normalized with respect to stability of the protein in the absence of added NaCl ($\Delta\Delta G = \Delta G_{[NaCl]} - \Delta G_{water}$). The curves through the data are only meant to guide the eye.

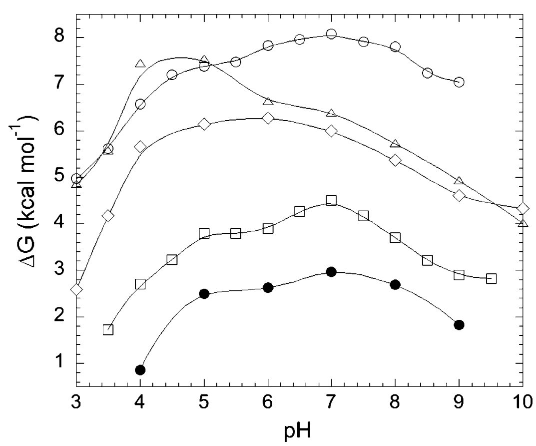

FIGURE 5: Conformational stability, ΔG (25 °C), of *Oi*- (●), *Bs*- (□), *St*- (◇), *Bh*- (△), and *Bst*HPr (○) proteins as a function of pH. Urea denaturation experiments were used to measure stability of the proteins at different pH at 25 °C. The curves through the data are meant only to guide the eye.

5. On the acidic side of the maximum, all HPr homologues are destabilized by ∼3 kcal mol^{-1}. In the alkaline pH range, however, there is more heterogeneity; *Bh*HPr (triangles in Figure 5) is most destabilized (by 3.5 kcal mol^{-1}) when the pH is increased from 5 to 10, and *Bst*HPr (circles in Figure 5) is least destabilized (by 1 kcal mol^{-1}) when the pH is increased from 7 to 10.

A Transferable Salt-Bridge Interaction from OiHPr. The sequence alignments for HPr homologues (Figure 1) show that on average the proteins share a 65% identity with *Bs*HPr. One notable difference is that *Oi*HPr has a Lys at position 2, while other homologues have an Ala. In a modeled structure (*49*), Lys 2 appears to form a salt bridge with Glu71. To test if this interaction can be transferred to and stabilize the mesophilic homologue *Bs*HPr, mutations were made at corresponding positions in *Bs*HPr (A2K+N71E). The stability measurements for the double variant, shown in Table 3, show that the interaction does stabilize *Bs*HPr by 1.1 kcal mol^{-1}. Further modeling suggested that an Arg at position 2 would form a better salt bridge in the *Bs*HPr protein. In fact, the A2R+N71E variant was indeed more stable (1.6 kcal

Table 3: Parameters Characterizing the Stability of *Bs*HPr Variants[a]

protein	urea denaturation ΔG (kcal mol^{-1})	urea denaturation m value[b] (kcal mol^{-1} M^{-1})	GuHCl denaturation ΔG (kcal mol^{-1})	GuHCl denaturation m value[c] (kcal mol^{-1} M^{-1})	$\Delta\Delta G_{\text{urea}-\text{GuHCl}}$ (kcal mol^{-1})	$\Delta\Delta G_{\text{WT}-\text{mut}}$[d] (kcal mol^{-1})	thermal denturation T_m (°C)	thermal denturation ΔH_m[e] (kcal mol^{-1})
***Bs*HPr**	5.0 (±0.2)	1.08	3.4 (±0.1)	3.28	1.6	−	73.0 (±0.6)	77
***Bs*2K71E**	6.1 (±0.4)	0.95	4.5 (±0.2)	3.37	1.4	−1.1	79.6 (±1.3)	85
***Bs*2R71E**	6.6 (±0.4)	0.99	4.9 (±0.2)	3.39	1.7	−1.6	83.1 (±2.3)	91

[a] All experiments were done in 10 mM sodium phosphate buffer at pH 7; solvent denaturation experiments were performed at 25 °C. All values reported are averages of results from multiple experiments, and the values in parentheses are the measured standard deviations. [b] Standard deviations for m value from urea denaturations ≤5%. [c] Standard deviations for m value from GuHCl denaturations ≤5%. [d] The difference in ΔG obtained from urea denaturations for mutant from the wild-type protein. [e] Standard deviations in ΔH_m were usually ≤10% of the average value reported.

mol^{-1}), suggesting that the ion-pair interaction is stabilizing and transferable between homologues.

DISCUSSION

Studies of proteins from extremophiles may provide unique insights into the forces involved in protein stability. The environmental stresses exerted on these proteins cause them to adapt in ways that are not seen in proteins from organisms inhabiting moderate environments. Thermophiles are of special interest because proteins from these organisms have adapted to the elevated habitat temperatures, which, unlike other environmental stresses, cannot be easily circumvented by compensatory mechanisms such as those proposed to regulate pH or ionic strength. Here, we have presented a thermodynamic characterization of five HPr homologues derived from organisms inhabiting diverse environments. The HPr homologues show substantial diversity in their thermal stability as demonstrated by their broad range of T_m values (Table 1). The T_m values of all homologues except *Oi*HPr correlate well with the habitat temperature of the organisms (T_E). For example, the most thermostable homologue, *Bst*HPr, derived from *B. staerothermophilus* has the highest habitat temperature (65 °C).

In addition to measurements of the thermal stability, we have also constructed complete stability curves for each of the proteins. Thus, we can calculate the conformational stability at any temperature in addition to estimates of other cardinal thermodynamic parameters. Comparisons of protein stability curves can, therefore, provide a thermodynamic description for the higher thermostability exhibited by proteins from thermophiles. Nojima et al. (*50*) first proposed three methods a thermophilic protein could employ to attain a higher T_m. These include stabilization by (1) a higher overall ΔG, (2) a lower ΔC_p, or (3) an elevated T_S. In a recent literature survey, we found that stabilization by a higher overall ΔG was the mechanism most often used in a set of 26 protein homologues (Razvi and Scholtz, submitted). Stability curves for our HPr homologues show that these proteins use this common method to attain a higher T_m as the stability curves are shifted to either higher or lower ΔG values without any significant changes in ΔC_p or T_S.

The stability curves for HPr homologues also reveal a very similar ΔG_E or free energy of stabilization at habitat temperature T_E (Table 2). The only exception is *Oi*HPr, probably because we have not correctly reproduced the high salinity and pH required for optimal stability of this extremely haloalkaliphilic organism. The similarity of the ΔG_E values for the HPr homologues is especially notable considering the diversity of habitat conditions represented and the number of different homologues. In the literature survey discussed above, we found only one case where ΔG_E values were reported for more than two homologues (four archaeal histone proteins were compared (*51*)), and the ΔG_E values were quite varied. The similar ΔG_E values for our HPr homologues strongly support the corresponding state hypothesis, which was first proposed by Somero (*52*) to explain stability of proteins from extremophiles. This hypothesis states that proteins balance their conformational stability with a need to be flexible, since flexibility is crucial to catalysis and other structural fluctuations required for protein function (*53*−*58*). Conformational stability, on the other hand, promotes rigidity in protein structures by increasing the number of stabilizing interactions, such as hydrogen bonds, hydrophobic interactions, and ion-pair interactions. The similarity of ΔG_E values for the HPr homologues supports this hypothesis, where these proteins appear to have tuned their thermodynamic characteristics to provide for nearly identical stability in each of their habitats.

The higher overall ΔG exhibited by some HPr homologues are most likely a result of an increased number of these stabilizing interactions; however, the molecular details cannot be delineated without high-resolution structures for all homologues. In the absence of structures, however, we can investigate some features such as the differences in general electrostatic interactions and possible changes in the accessible surface area upon unfolding (ΔASA) between homologues. The ΔC_p values determined for the HPr proteins are very similar, as expected for proteins of similar size, and point to very similar ΔASA values for all homologues. Likewise, the m values from solvent denaturation experiments, which correlate with the size of a protein and the amount of surface area it exposes upon unfolding (*59*), are accordingly similar for most HPr homologues, except *Oi*HPr which has a slightly higher value. Therefore, the ΔASA for our HPr homologues are quite similar unlike in the case of RNase H homologues, where it was found that the thermophilic homologue has a structured cluster in the denatured state and thus a lower ΔASA as reflected in decreased ΔC_p (*25*, *60*, *61*).

In some statistical surveys comparing proteins from mesophiles and thermophiles (*62*, *63*), the most prevalent feature of proteins from thermophiles that shows a positive correlation with growth temperature is the number of electrostatic interactions. Proteins from thermophiles were found to have a higher number of surface-charged groups involved in stabilizing interactions such as salt bridges and side-chain hydrogen bonds (*64*−*68*). Similarly, statistical surveys comparing sequences of halophilic and mesophilic proteins have found an increased number of acidic residues in halophilic proteins (*69*). This is not surprising given the established role of acidic residues, especially Glu, that are capable of binding more water than other residues. This helps create a hydration shell that keeps the protein solvated in high salt conditions, where other proteins lacking excess negative charges would aggregate (*70*−*72*). Accordingly, sequence comparison of *Oi*HPr, the extremely halophilic HPr homologue, with other homologues shows that the number of acidic residues is the highest in *Oi*HPr (14 Asp and Glu residues), compared with other homologues, which have 10 (*Bst*HPr), 11 (*St*HPr), or 12 (*Bh*- and *Bs*HPr). To determine if electrostatic interactions are important in the differential stabilities of the HPr proteins, we have measured protein stability for all the HPr homologues in different solution conditions by varying ionic strength or pH. We have also used the differences in stability measured by urea and GuHCl denaturation experiments ($\Delta\Delta G_{\mathrm{urea-GuHCl}}$) for a protein as a first approximation of electrostatic forces, as has been used in the past (*73*).

The HPr proteins show a common trend in changes in stability with added NaCl, the prominent outlier being *Bs*HPr, which is more destabilized than other homologues in low NaCl concentration. This suggests, rather counter intuitively, that the mesophilic homologue has more optimized electrostatic interactions which can be screened at low NaCl concentration, thus, destabilizing the protein to a greater extent than thermophilic homologues such as *Bst*- and *St*HPr. General electrostatic interactions can also be investigated by comparing how the stability changes with pH. pH perturbations can affect protein stability by causing changes in ionization states of side-chain groups involved in favorable or unfavorable interactions. A comparison of such data for the HPr homologues shows that most homologues have a similar response to change in pH with destabilization in both acidic and basic pH domains and maximum stability at neutral pH. The exceptions are *St*- and *Bh*HPr, which have maximal stabilities in slightly acidic conditions. Finally, when the $\Delta\Delta G_{\mathrm{urea-GuHCl}}$ values are compared, we find that the HPr homologues fall into mainly one group, with *Bs*-, *Bst*-, and *Bh*HPr having similar values. *St*HPr has a lower $\Delta\Delta G_{\mathrm{urea-GuHCl}}$, and *Oi*HPr has a higher value; in the case of *Oi*HPr, we attribute this to the ΔG estimate from GuHCl denaturation data, which might be suspect due to the paucity of data in the pretransition region at 25 °C. Thus, a common trend that emerges when looking at data discussed above is that all HPr proteins have similar contributions from electrostatic interactions, and *St*HPr is consistently an outlier in all three types of experiments performed. In the absence of high-resolution structures for all homologues, these data indicate that increased ΔG of some homologues is probably not a result of enhanced contributions from electrostatic interactions.

The structural and sequence comparisons between pairs of proteins derived from mesophiles and thermophiles have proven indispensable in comparative studies of the kind we have undertaken here (for a recent example see ref *28*). Structural comparisons can reveal stabilizing interactions, which may be more plentiful in the thermophilic homologue. A structural comparison between two of the five HPr homologues for which structures are available was reported earlier (Table 3 in ref *38*). It was found that the two proteins have very similar structures with very similar number of hydrogen bonds, salt-bridge interactions, and buried polar and apolar surface area within errors of estimation and the resolution of the structures. A superposition of Cα chains for these homologues from *Bs* and *Bst* (Figure 1) depicts the high structural similarity observed between a mesophilic and the most thermophilic HPr in our group. However, a sequence comparison combined with structural modeling for *Oi*HPr has revealed a salt-bridge interaction between residues 2 and 71, which we were able to transfer to the *Bs*HPr protein, resulting in significant stabilization (Table 2). This suggests that detailed comparisons such as those presented here will be useful in identifying potential molecular interactions that can be transferred between protein homologues and optimized for enhanced stability.

We have presented here a detailed characterization of five HPr homologues derived from organisms inhabiting quite diverse environments as a step toward understanding the origins of their varied stability behaviors. To our knowledge, this is one of the few studies that provide thermodynamic characterization of protein homologues derived from temperature, high salinity, and pH-adapted organisms. We have also established a thermodynamic mechanism employed by these proteins to enhance their T_m. To some level of certainty, electrostatic interactions have been ruled out as the cause of enhanced stabilities of thermophilic homologues. Sequence and structural comparisons were able to identify a transferable stabilizing interaction, and with the aid of more structural information, we hope to identify key interactions responsible for enhanced stability of thermophilic homologues and to determine how easily these interactions can be transferred to homologous proteins

ACKNOWLEDGMENT

We thank Dr. Lonnie Ingram, University of Florida, Gainesville, FL, for the plasmid for expression of *Bst*HPr. We thank Jennifer Dulin for her help at various stages of the project. We also thank Dr. Mohammad Mohammad for his help in cloning the *Bh*HPr gene.

REFERENCES

1. Anfinsen, C. B., Haber, E., Sela, M., and White, F. H., Jr. (1961) The kinetics of formation of native ribonuclease during oxidation of the reduced polypeptide chain, *Proc. Natl. Acad. Sci. U.S.A. 47*, 1309−1314.
2. Anfinsen, C. B. (1973) Principles that govern the folding of protein chains, *Science 181*, 223−230.
3. Sterner, R., and Liebl, W. (2001) Thermophilic adaptation of proteins, *Crit. Rev. Biochem. Mol. Biol. 36*, 39−106.
4. Jaenicke, R. (1998) What ultrastable globular proteins teach us about protein stabilization, *Biochemistry (Moscow, Russ. Ed.) 63*, 312−321.
5. Vieille, C., and Zeikus, J. G. (1996) Thermozymes: identifying molecular determinants of protein structural and functional stability, *Trends Biotechnol. 14*, 183−190.
6. Rees, D. C., and Adams, M. W. (1995) Hyperthermophiles: taking the heat and loving it, *Structure 3*, 251−254.
7. Somero, G. N. (1995) Proteins and temperature, *Annu. Rev. Physiol. 57*, 43−68.
8. Argos, P., Rossman, M. G., Grau, U. M., Zuber, H., Frank, G., and Tratschin, J. D. (1979) Thermal stability and protein structure, *Biochemistry 18*, 5698−5703.
9. Bougault, C. M., Eidsness, M. K., and Prestegard, J. H. (2003) Hydrogen bonds in rubredoxins from mesophilic and hyperthermophilic organisms, *Biochemistry 42*, 4357−4372.

10. Tanner, J. J., Hecht, R. M., and Krause, K. L. (1996) Determinants of enzyme thermostability observed in the molecular structure of *Thermus aquaticus* D-glyceraldehyde-3-phosphate dehydrogenase at 2.5 Å resolution, *Biochemistry 35*, 2597−2609.
11. Britton, K. L., Baker, P. J., Borges, K. M., Engel, P. C., Pasquo, A., Rice, D. W., Robb, F. T., Scandurra, R., Stillman, T. J., and Yip, K. S. (1995) Insights into thermal stability from a comparison of the glutamate dehydrogenases from *Pyrococcus furiosus* and *Thermococcus litoralis*, *Eur. J. Biochem. 229*, 688−695.
12. Perl, D., Mueller, U., Heinemann, U., and Schmid, F. X. (2000) Two exposed amino acid residues confer thermostability on a cold shock protein, *Nat. Struct. Biol. 7*, 380−383.
13. Criswell, A. R., Bae, E., Stec, B., Konisky, J., and Phillips, G. N., Jr. (2003) Structures of thermophilic and mesophilic adenylate kinases from the genus *Methanococcus*, *J. Mol. Biol. 330*, 1087−1099.
14. Petsko, G. A. (2001) Structural basis of thermostability in hyperthermophilic proteins, or "there's more than one way to skin a cat", *Methods Enzymol. 334*, 469−478.
15. Jaenicke, R. (1991) Protein stability and molecular adaptation to extreme conditions, *Eur. J. Biochem. 202*, 715−728.
16. Booth, I. R. (1985) Regulation of cytoplasmic pH in bacteria, *Microbiol. Rev. 49*, 359−378.
17. Yancey, P. H., Clark, M. E., Hand, S. C., Bowlus, R. D., and Somero, G. N. (1982) Living with water stress: evolution of osmolyte systems, *Science 217*, 1214−1222.
18. Timasheff, S. N. (1993) The control of protein stability and association by weak interactions with water: how do solvents affect these processes? *Annu. Rev. Biophys. Biomol. Struct. 22*, 67−97.
19. Timasheff, S. N. (2002) Protein hydration, thermodynamic binding, and preferential hydration, *Biochemistry 41*, 13473−13482.
20. Horikoshi, K. (1999) Alkaliphiles: some applications of their products for biotechnology, *Microbiol. Mol. Biol. Rev. 63*, 735−750.
21. Vieille, C., and Zeikus, G. J. (2001) Hyperthermophilic enzymes: sources, uses, and molecular mechanisms for thermostability, *Microbiol. Mol. Biol. Rev. 65*, 1−43.
22. Arnold, F. H., Wintrode, P. L., Miyazaki, K., and Gershenson, A. (2001) How enzymes adapt: lessons from directed evolution, *Trends Biochem. Sci. 26*, 100−106.
23. Wintrode, P. L., and Arnold, F. H. (2000) Temperature adaptation of enzymes: lessons from laboratory evolution, *Adv. Protein Chem. 55*, 161−225.
24. Van den Burg, B., Vriend, G., Veltman, O. R., Venema, G., and Eijsink, V. G. (1998) Engineering an enzyme to resist boiling, *Proc. Natl. Acad. Sci. U.S.A. 95*, 2056−2060.
25. Hollien, J., and Marqusee, S. (1999) A thermodynamic comparison of mesophilic and thermophilic ribonucleases H, *Biochemistry 38*, 3831−3836.
26. Deutschman, W. A., and Dahlquist, F. W. (2001) Thermodynamic basis for the increased thermostability of CheY from the hyperthermophile *Thermotoga maritima*, *Biochemistry 40*, 13107−13113.
27. Lee, C. F., Allen, M. D., Bycroft, M., and Wong, K. B. (2005) Electrostatic interactions contribute to reduced heat capacity change of unfolding in a thermophilic ribosomal protein l30e, *J. Mol. Biol. 348*, 419−431.
28. Cheung, Y. Y., Lam, S. Y., Chu, W. K., Allen, M. D., Bycroft, M., and Wong, K. B. (2005) Crystal structure of a hyperthermophilic archaeal acylphosphatase from *Pyrococcus horikoshii*−structural insights into enzymatic catalysis, thermostability, and dimerization, *Biochemistry 44*, 4601−4611.
29. Kreig, N. R., and Holt, J. G. (1984) *Bergey's Manual of Systematic Bacteriology*, 1st ed., Vol. 2, Williams & Wilkins, Baltimore, MD.
30. Esser, A. F., and Souza, K. A. (1974) Correlation between thermal death and membrane fluidity in *Bacillus stearothermophilus*, *Proc. Natl. Acad. Sci. U.S.A. 71*, 4111−4115.
31. Takami, H., Nakasone, K., Takaki, Y., Maeno, G., Sasaki, R., Masui, N., Fuji, F., Hirama, C., Nakamura, Y., Ogasawara, N., Kuhara, S., and Horikoshi, K. (2000) Complete genome sequence of the alkaliphilic bacterium*Bacillus halodurans* and genomic sequence comparison with *Bacillus subtilis*, *Nucleic Acids Res. 28*, 4317−4331.
32. Takami, H., and Horikoshi, K. (1999) Reidentification of facultatively alkaliphilic *Bacillus* sp. C-125 to *Bacillus halodurans*, *Biosci. Biotechnol. Biochem. 63*, 943−945.
33. Lu, J., Nogi, Y., and Takami, H. (2001) *Oceanobacillus iheyensis* gen. nov., sp. nov., a deep-sea extremely halotolerant and alkaliphilic species isolated from a depth of 1050 m on the Iheya Ridge, *FEMS Microbiol. Lett. 205*, 291−297.
34. Meadow, N. D., Fox, D. K., and Roseman, S. (1990) The bacterial phosphoenolpyruvate: glycose phosphotransferase system, *Annu. Rev. Biochem. 59*, 497−542.
35. Scholtz, J. M. (1995) Conformational stability of HPr: the histidine-containing phosphocarrier protein from *Bacillus subtilis*, *Protein Sci. 4*, 35−43.
36. Nicholson, E. M., and Scholtz, J. M. (1996) Conformational stability of the *Escherichia coli* HPr protein: test of the linear extrapolation method and a thermodynamic characterization of cold denaturation, *Biochemistry 35*, 11369−11378.
37. Van Nuland, N. A., Meijberg, W., Warner, J., Forge, V., Scheek, R. M., Robillard, G. T., and Dobson, C. M. (1998) Slow cooperative folding of a small globular protein HPr, *Biochemistry 37*, 622−637.
38. Sridharan, S., Razvi, A., Scholtz, J. M., and Sacchettini, J. C. (2005) The HPr proteins from the thermophile *Bacillus stearothermophilus* can form domain-swapped dimers, *J. Mol. Biol. 346*, 919−931.
39. Herzberg, O., Reddy, P., Sutrina, S., Saier, M. H., Jr., Reizer, J., and Kapadia, G. (1992) Structure of the histidine-containing phosphocarrier protein HPr from *Bacillus subtilis* at 2.0 Å resolution, *Proc. Natl. Acad. Sci. U.S.A. 89*, 2499−2503.
40. Anderson, J. W., Bhanot, P., Georges, F., Klevit, R. E., and Waygood, E. B. (1991) Involvement of the carboxy-terminal residue in the active site of the histidine-containing protein, HPr, of the phosphoenolpyruvate: sugar phosphotransferase system of *Escherichia coli*, *Biochemistry 30*, 9601−9607.
41. Lai, X., and Ingram, L. O. (1995) Discovery of a ptsHI operon, which includes a third gene (ptsT), in the thermophile *Bacillus stearothermophilus*, *Microbiology 141* (Pt. 6), 1443−1449.
42. Howorka, S., and Bayley, H. (1998) Improved protocol for high-throughput cysteine scanning mutagenesis, *BioTechniques 25*, 764−772.
43. Kalia, A., Rattan, A., and Chopra, P. (1999) A method for extraction of high-quality and high-quantity genomic DNA generally applicable to pathogenic bacteria, *Anal. Biochem. 275*, 1−5.
44. Waygood, E. B., Reiche, B., Hengstenberg, W., and Lee, J. S. (1987) Characterization of mutant histidine-containing proteins of the phosphoenolpyruvate:sugar phosphotransferase system of *Escherichia coli* and *Salmonella typhimurium*, *J. Bacteriol. 169*, 2810−2818.
45. Grimsley, G. R., Huyghues-Despointes, B. M. P., Pace, C. N., and Scholtz, J. M. (2003) Measuring the conformational stability of a protein, in *Purifying Proteins for Proteomics: A Laboratory Manual* (Simpson, R. J., Ed.) pp 535−566, Cold Spring Harbor Press, Cold Spring Harbor, NY.
46. Becktel, W. J., and Schellman, J. A. (1987) Protein stability curves, *Biopolymers 26*, 1859−1877.
47. Pace, C. N., and Laurents, D. V. (1989) A new method for determining the heat capacity change for protein folding, *Biochemistry 28*, 2520−2525.
48. Thompson, J. D., Higgins, D. G., and Gibson, T. J. (1994) CLUSTAL W: improving the sensitivity of progressive multiple sequence alignment through sequence weighting, position-specific gap penalties and weight matrix choice, *Nucleic Acids Res. 22*, 4673−4680.
49. Guex, N., and Peitsch, M. C. (1997) SWISS-MODEL and the Swiss-PdbViewer: an environment for comparative protein modeling, *Electrophoresis 18*, 2714−2723.
50. Nojima, H., Ikai, A., Oshima, T., and Noda, H. (1977) Reversible thermal unfolding of thermostable phosphoglycerate kinase. Thermostability associated with mean zero enthalpy change, *J. Mol. Biol. 116*, 429−442.
51. Li, W. T., Grayling, R. A., Sandman, K., Edmondson, S., Shriver, J. W., and Reeve, J. N. (1998) Thermodynamic stability of archaeal histones, *Biochemistry 37*, 10563−10572.
52. Somero, G. N. (1978) Temperature adaptation of enzymes−biological optimization through structure−function compromises, *Annu. Rev. Ecol. Syst. 9*, 1−29.
53. Zavodszky, P., Kardos, J., Svingor, and Petsko, G. A. (1998) Adjustment of conformational flexibility is a key event in the thermal adaptation of proteins, *Proc. Natl. Acad. Sci. U.S.A. 95*, 7406−7411.
54. Jaenicke, R. (2000) Do ultrastable proteins from hyperthermophiles have high or low conformational rigidity? *Proc. Natl. Acad. Sci. U.S.A. 97*, 2962−2964.

55. Akke, M. (2004) Out of hot water, *Nat. Struct. Mol. Biol. 11*, 912−913.
56. Wolf-Watz, M., Thai, V., Henzler-Wildman, K., Hadjipavlou, G., Eisenmesser, E. Z., and Kern, D. (2004) Linkage between dynamics and catalysis in a thermophilic-mesophilic enzyme pair, *Nat. Struct. Mol. Biol. 11*, 945−949.
57. Eisenmesser, E. Z., Millet, O., Labeikovsky, W., Korzhnev, D. M., Wolf-Watz, M., Bosco, D. A., Skalicky, J. J., Kay, L. E., and Kern, D. (2005) Intrinsic dynamics of an enzyme underlies catalysis, *Nature 438*, 117−121.
58. Varley, P. G., and Pain, R. H. (1991) Relation between stability, dynamics and enzyme activity in 3-phosphoglycerate kinases from yeast and *Thermus thermophilus*, *J. Mol. Biol. 220*, 531−538.
59. Myers, J. K., Pace, C. N., and Scholtz, J. M. (1995) Denaturant m values and heat capacity changes: relation to changes in accessible surface areas of protein unfolding, *Protein Sci. 4*, 2138−2148.
60. Guzman-Casado, M., Parody-Morreale, A., Robic, S., Marqusee, S., and Sanchez-Ruiz, J. M. (2003) Energetic evidence for formation of a pH-dependent hydrophobic cluster in the denatured state of *Thermus thermophilus* ribonuclease H, *J. Mol. Biol. 329*, 731−743.
61. Robic, S., Guzman-Casado, M., Sanchez-Ruiz, J. M., and Marqusee, S. (2003) Role of residual structure in the unfolded state of a thermophilic protein, *Proc. Natl. Acad. Sci. U.S.A. 100*, 11345−11349.
62. Chakravarty, S., and Varadarajan, R. (2002) Elucidation of factors responsible for enhanced thermal stability of proteins: a structural genomics based study, *Biochemistry 41*, 8152−8161.
63. Szilagyi, A., and Zavodszky, P. (2000) Structural differences between mesophilic, moderately thermophilic and extremely thermophilic protein subunits: results of a comprehensive survey, *Structure 8*, 493−504.
64. Karshikoff, A., and Ladenstein, R. (2001) Ion pairs and the thermotolerance of proteins from hyperthermophiles: a "traffic rule" for hot roads, *Trends Biochem. Sci. 26*, 550−556.
65. Xiao, L., and Honig, B. (1999) Electrostatic contributions to the stability of hyperthermophilic proteins, *J. Mol. Biol. 289*, 1435−1444.
66. Spassov, V. Z., Karshikoff, A. D., and Ladenstein, R. (1995) The optimization of protein−solvent interactions: thermostability and the role of hydrophobic and electrostatic interactions, *Protein Sci. 4*, 1516−1527.
67. Perutz, M. F. (1978) Electrostatic effects in proteins, *Science 201*, 1187−1191.
68. Elcock, A. H. (1998) The stability of salt bridges at high temperatures: implications for hyperthermophilic proteins, *J. Mol. Biol. 284*, 489−502.
69. Fukuchi, S., Yoshimune, K., Wakayama, M., Moriguchi, M., and Nishikawa, K. (2003) Unique amino acid composition of proteins in halophilic bacteria, *J. Mol. Biol. 327*, 347−357.
70. Kuntz, I. D., Jr., and Kauzmann, W. (1974) Hydration of proteins and polypeptides, *Adv. Protein Chem. 28*, 239−345.
71. Dym, O., Mevarech, M., and Sussman, J. L. (1995) Structural features that stabilize halophilic malate dehydrogenase from an archaebacterium, *Science 267*, 1344−1346.
72. Rao, J. K., and Argos, P. (1981) Structural stability of halophilic proteins, *Biochemistry 20*, 6536−6543.
73. Kohn, W. D., Kay, C. M., and Hodges, R. S. (1995) Protein destabilization by electrostatic repulsions in the two-stranded alpha-helical coiled-coil/leucine zipper, *Protein Sci. 4*, 237−250.

BI060038+